Technical University of Denmark

DTU

Dynamic stiffness of horizontally vibrating suction caissons

Latini, Chiara; Zania, Varvara; Cisternino, Michele

Link back to DTU Orbit

DTU Library
Technical Information Center of Denmark

NGM 2016 Reykjavik
Proceedings of the 17th Nordic Geotechnical Meeting
Challenges in Nordic Geotechnic   25th – 28th of May

Dynamic stiffness of horizontally vibrating suction caissons

C. Latini
Civil Engineering Department, Technical University of Denmark, Lyngby, Denmark,
chila@byg.dtu.dk

V. Zania
Civil Engineering Department, Technical University of Denmark, Lyngby, Denmark,

M. Cisternino
Civil Engineering Department, Technical University of Denmark, Lyngby, Denmark,

ABSTRACT

The promising potential for offshore wind market is on developing wind farms in deeper waters with bigger turbines. In deeper waters the design foundation configuration may consist of jacket structures supported by floating piles or by suction caissons. Taking the soil-structure interaction effects into consideration requires the prior estimation of the dynamic impedances of the foundation. Even though numerous studies exist for piles, only limited number of publications can be found for suction caissons subjected to dynamic loads. Therefore, the purpose of this study is to examine the dynamic response of this type of foundation using the finite element method (FEM) to account for the interaction with the soil. 3D numerical models for both the soil and the suction caisson are formulated in a frequency domain. The response of the soil surrounding the foundation is considered linear viscoelastic with hysteretic type damping. In addition, non-reflective boundaries are included in the model. Two different soil profiles are presented, one when the rigid bedrock is set close to the seabed and the other one when it is far away.
The dynamic impedances at the top of the foundation are determined and compared to existing analytical solutions suggested for piles. Relatively good agreement has been achieved comparing the numerical results with the analytical solutions. Then, the effect of the soil layer shear wave velocity on the dynamic stiffness coefficients is analysed. The results have indicated that increasing the stiffness of the soil stratum the dynamic impedances grow, while the damping reduces in the frequency range investigated.

Keywords: soil-structure interaction, dynamic stiffness, damping, suction caissons, numerical modelling

1 INTRODUCTION

The offshore wind market is progressing by developing wind turbines with larger rotors and higher capacity generators, in order to deploy deep offshore designs. It is fundamental to assess the resonance frequencies of the wind turbine structure accurately in order to avoid the first resonance frequency of the wind turbines coinciding to the excitation frequencies of the rotor system as delineated in DNV-OS-J101 (2004). In addition, the effect of the soil-foundation-structure interaction should be included in the estimation of the natural vibration characteristics of the OWTs as indicated by several studies (Adhikari and Bhattacharya, 2012; Alexander and Bhattacharya, 2011; Zania, 2014). The majority of installed or operating turbines are supported on fixed foundation system (Bhattacharya, 2014), while deep installations require jackets structures with

floating piles or with suction caissons. In the past, suction caissons have been deployed as anchors or as foundations for offshore platforms. According to Houlsby et al. (2005), suction caissons can be adopted as offshore wind turbine foundations embedded in suitable soil conditions and especially for deeper waters installation, of water depth of approximately up to 40m.

Suction caissons differ from other foundation types such as piles, regarding the installation procedure applied offshore and the geometric properties including the rigid cap and the lateral flexibility (with slenderness ratio lower than 4). Contrary to offshore pile driving, heavy duty equipment is not required in the process of suction caisson installation, which is materialized by using self-weight and suction as the driving forces (Byrne and Houlsby, 2006). This becomes a considerable advantage in the case of deep water installations.

In the literature the problem of the dynamic soil-pile interaction has been extensively investigated. Considering only the studies for linear elastic soil layer, they can be briefly categorized into analytical solutions (Novak and Nogami, 1977; Mylonakis, 2001; Nozoe et al., 1985; Latini et al., 2015) and numerical finite element solutions (Velez et al., 1983; Gazetas, 1984). On the other hand, the dynamic response of suction caissons received less attention (Liingaard, 2006). In the work of Liingaard (2006) the dynamic stiffness coefficients were determined, considering linear viscoelastic soil and modelling the suction caisson using a coupled BE/FE model in homogeneous halfspace comparing the obtained results with analytical solutions for surface foundations.

The purpose of the current study is to investigate the dynamic response of suction caissons for the estimation of the dynamic stiffness and damping coefficients with respect to the frequency. Therefore, 3D FE models were developed and the dynamic impedances to lateral loading were estimated. The results of the numerical models have been compared respectively with the rigorous analytical solution of soil-end bearing pile vibration by Novak et al. (1977) and the analytical solution proposed for floating piles by Latini et al. (2015). The effect of the stiffness of the soil on the soil-caisson system response is further discussed.

2 METHODOLOGY

3D finite element models have been developed to investigate the dynamic impedances of the suction caisson in the commercial software ABAQUS (Simulia, 2013). The numerical models account for the following hypotheses: 1) linear elastic isotropic behaviour of the suction caisson; 2) linear viscoelastic isotropic behaviour of soil with hysteretic type damping and 3) perfect contact between the foundation and the soil during the analysis.

Due to the symmetry of the problem, only half of the foundation and the surrounding soil are taken into account. The suction caisson consists of steel with diameter d=5m, skirt length H=10m, Young's modulus E_p = 210 GPa and Poisson's ratio ν=0.35. The foundation skirt and the cap of the caisson have respectively thickness of t_{skirt}=d/100 and t_{cap}=5t_{skirt}.

Three different suction caisson modelling approaches are presented: 1) shell pile, where the foundation is modelled by shell; 2) caisson with cap; and 3) equivalent solid pile, for which equivalent material properties are applied to match the bending stiffness.

The soil surrounding the foundation has hysteretic type damping of ζ=5.0% and constant profile of shear wave velocity V_s=250-400m/s. Hexahedral elements are used to discretize the soil domain of diameter 24d and height H_s=6d=30m. Infinite elements are placed at the boundaries in order to model the far field soil and avoid spurious reflection. The soil and the foundation skirt and the caisson cap are tied together in order to satisfy the displacement compatibility.

Steady state linearized response of the model subject to harmonic excitation in the frequency domain is performed. The dynamic impedances K_{su}, $K_{s\theta}$, K_{mu} and $K_{m\theta}$ at the level of the pile head are then calculated as shear forces, S, and moments, M, when the head of the suction caisson is subjected to unit displacement, u, and rotation, θ. The mesh size needs to be small enough to capture the

stress wave accurately. A mesh size of at least 10 to 20 elements per wave length is assumed a good approximation for the frequency range of interest, including up to the third eigenfrequency of the soil layer $\alpha_0 = 5/2\pi$. Note that α_0 is a dimensionless frequency related to the eigenfrequency of the soil layer, since it is given as the product of the wave number and the height of the soil layer:

$$\alpha_0 = \frac{\omega H_s}{V_s} \qquad (1)$$

where ω(rad), H_s(m) and V_s(m/s) are respectively the circular frequency, the height and the shear wave velocity of the soil layer.
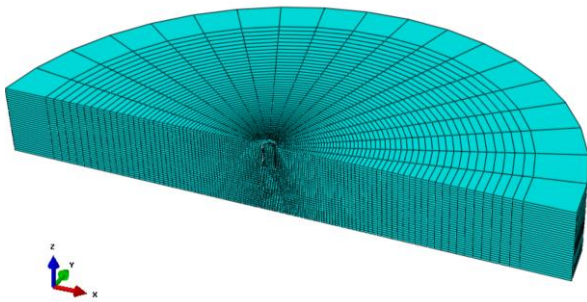A view of the model with the mesh refinement is shown in Figure 1.

Figure 1 Finite element model of the suction caisson and the surrounding soil.

3 NUMERICAL RESULTS

Two layered soil profile characterized by high stiffness contrast is analyzed. Then, 3D numerical models are developed considering different depths of the surface soil layer with respect to the length of the skirt of the caisson, see Figure 2. In the study the soil profile with height equal to the caisson skirt length is defined as profile 1, while the one with increased height as profile 2.
The results for profile 1 and profile 2 are compared respectively with the rigorous continuum analytical solution formulated for end bearing piles by Novak et al. (1977) and that for floating piles by Latini et al. (2015). The different suction caisson modelling procedures with shell elements and continuum elements are implemented in order to achieve a direct comparison with the analytical solutions. The effect of the

stiffness of the soil on the soil-caisson system response is further discussed, by considering stiffer soil formation.
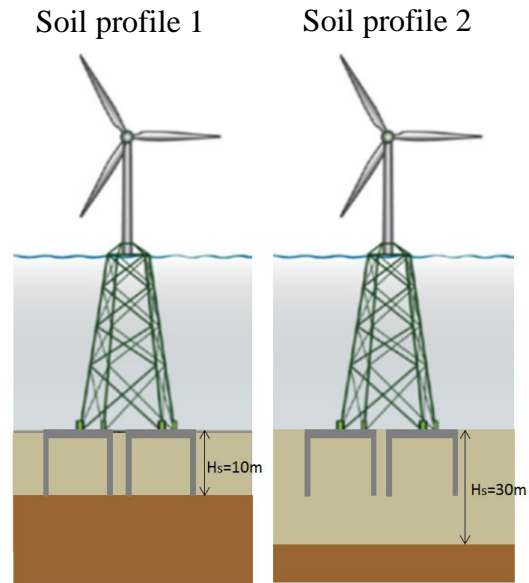

Figure 2 Illustration of the two soil profiles investigated in this study.

The dynamic component (real part of the complex valued stiffness terms divided by the corresponding static component K^0 and imaginary part of the complex valued stiffness terms divided by the corresponding dynamic component K_{xx}) of the three stiffness terms is presented with respect to the non-dimensional frequency α_0.
First the static stiffness coefficients of the different modelling approaches are calculated and presented in Table 1 for the soil profile 1, along with the corresponding ones obtained from the analytical solution.

Table 1 Static suction caisson stiffness obtained from the numerical models and the analytical solution of Novak et al. (1977) for profile 1.

	Ksu [kN]	Ksθ [kN]	Kmθ [kNm]
Caisson	4.656E+6	-1.223E+7	1.120E+8
Shell pile	5.010E+6	-1.410E+7	1.325E+8
Solid eq. pile	7.109E+6	-2.384E+7	1.731E+8
Novak et al. (1977)	8.845E+6	-3.441E+7	2.148E+8

The stiffness components of the caisson model slightly differ from those of the shell pile, while the difference is more significant with the solid equivalent pile regarding all

the components. In addition, it is observed that the results obtained from the numerical models are overestimated by the analytical solution, particularly regarding the translational and the cross coupling terms.

In Figures 3, 4 and 5, the real (K_{su}, $K_{s\theta}$, and $K_{m\theta}$) and the imaginary ($2\zeta_{su}$, $2\zeta_{s\theta}$, and $2\zeta_{m\theta}$) part of the dynamic impedances are shown. A common trend for all the stiffness components is the observed drop of stiffness at the 1st eigenfrequency of the soil layer ($\alpha_0=1/2\pi$). A change in the pattern slope is attained around the first vertical resonance $\alpha_0=1/2\pi\eta$, where $\eta = \sqrt{\frac{2(1-\nu)}{1-2\nu}}$, which is mainly observed for the translational and rocking component; whereas the cross coupling coefficient is characterized by an increase of stiffness at the same normalized frequency.
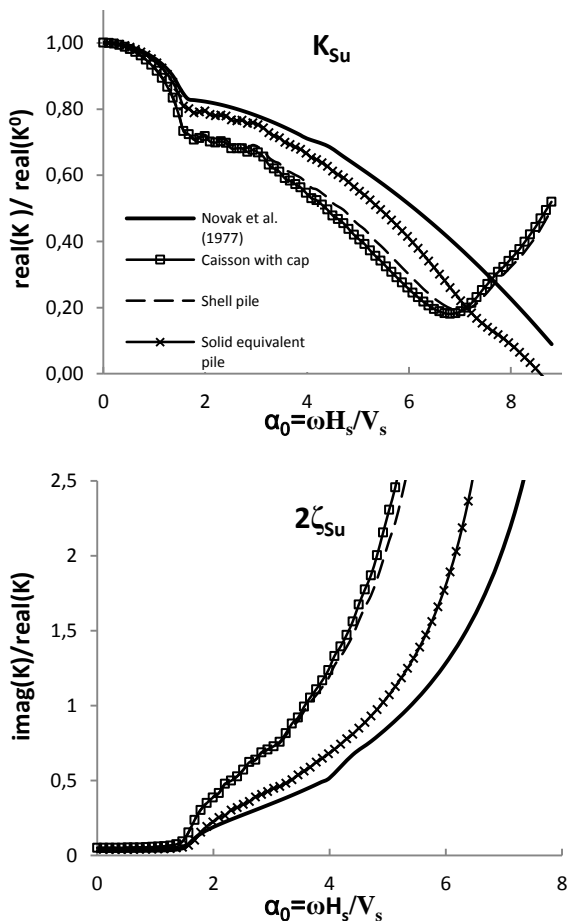

Figure 3 Variation of the translational stiffness and damping coefficients with respect to the dimensionless frequency for profile 1.

The intermediate frequency interval ($\alpha_0=1/2\pi\eta$-6) is characterized by a linearly

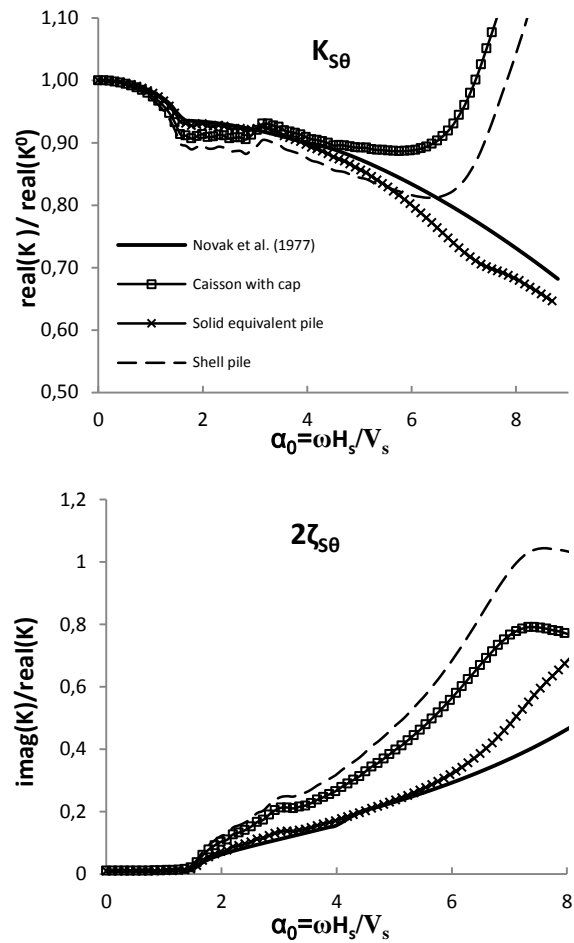decrease of the dynamic stiffness consistent for all the components.

Figure 4 Variation of the coupling stiffness and damping coefficients with respect to the dimensionless frequency for profile 1.

On the contrary, in the high frequency range the solid equivalent pile shows a softer behavior with monotonically decreasing pattern with respect to the other two models for all the components. This trend resembles the one suggested by the analytical solution, although the latter is not able to capture the 1st vertical resonance.
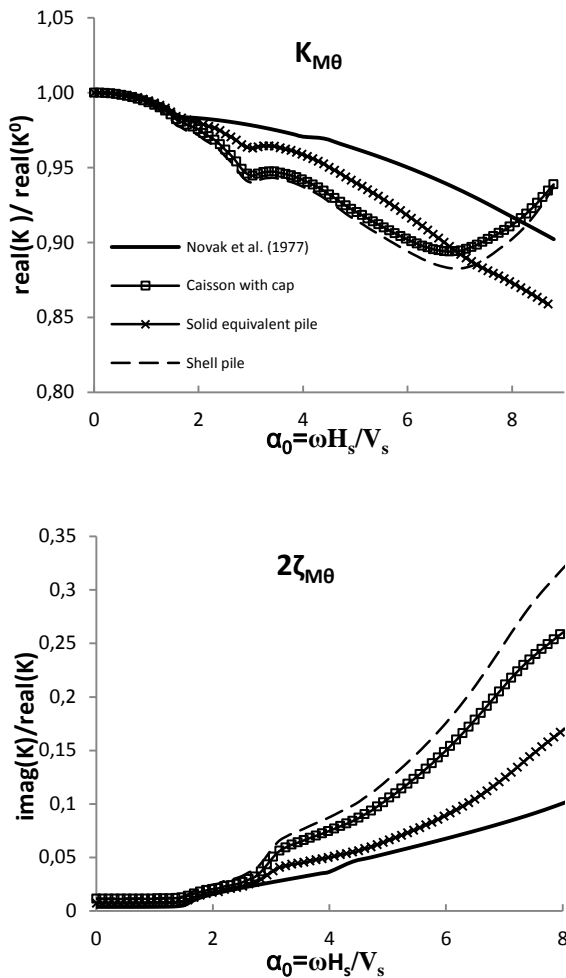
Figure 5 Variation of the rocking stiffness and damping coefficients with respect to the dimensionless frequency for profile 1

On the other hand the caisson and the shell pile model exhibit an exponential increase at the higher frequency range α_0=6.5-7. This is possibly attributed to the presence of a surface wave (Rayleigh wave). Indeed, the displacement contour plot at this frequency (Figure 6) shows that the soil within the foundation and surrounding it experiences a surface wave with wave length almost equal to the diameter of the caisson and displays the occurrence of the Rayleigh wave through the s-pattern on the soil surface propagating radially from the caisson.
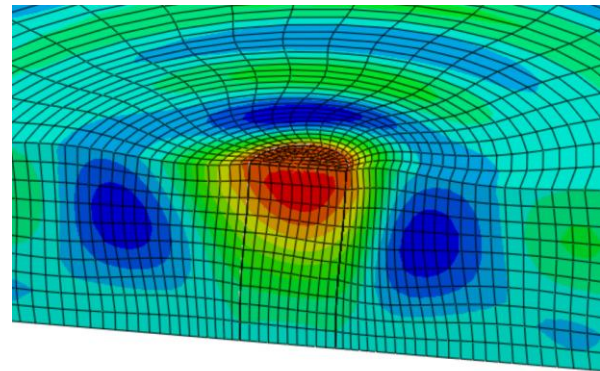

Figure 6 Displacement contour plot illustrating the presence of Rayleigh wave in the soil within the caisson.

The imaginary part of the dynamic component of the dynamic impedances, is associated with the generated damping due to soil-caisson interaction. The radiation damping is generated for frequencies higher than the first eigenfrequency of the soil layer for all the components, and this is demonstrated by the increasing values of the coefficients with frequency (Figure 3,4, and 5). In the case of a linear increase viscous type damping is generated. This type of behavior is observed over the intermediate frequency range (α_0=2-4). A slight change in the slope of the damping is also marked after each eigenfrequency of the soil layer.

Moreover, it might be concluded that the presence of the cap does not affect the dynamic response of the soil-caisson system for the translation and rocking component, since the dynamic response of the shell pile and the caisson match almost perfectly. On the other hand a significant effect is noticed on the coupling stiffness term after the 1st vertical resonance for both stiffness and damping coefficients. The analytical solution is overestimating the dynamic stiffness and underestimating the damping for all the components, however it is in relatively good agreement with the equivalent solid pile. This indicates that the inner soil affects the dynamic response of the caisson, by allowing wave propagation of smaller wave lengths.

The second soil profile describes a deep soil formation. For this case the response of the shell pile is not reported in the graphs, since it matches with the caisson case.

First the static stiffness coefficients were estimated and the results are presented in Table 2.

Table 2 Static suction caisson stiffness obtained from the numerical models and the analytical solution of Latini et al. (2015) for Profile 2.

	Ksu [kN]	Ksθ [kN]	Kmθ [kNm]
Caisson	3.220E+6	-9.237E+6	9.608E+7
Solid eq. pile	3.833E+6	-1.279E+7	1.191E+8
Latini et al. (2015)	4.288E+6	-1.529E+7	1.339E+8

The static stiffness coefficients of the solid equivalent pile are slight higher than those of the caisson model. The analytical solution suggests similar values to those obtained from the numerical models.

In Figures 7, 8 and 9, the real (K_{su}, $K_{s\theta}$, and $K_{m\theta}$) and the imaginary ($2\zeta_{su}$, $2\zeta_{s\theta}$, and $2\zeta_{m\theta}$) parts of the dynamic impedances are presented. A decrease of stiffness is marked after the 1st and 2nd horizontal eigenfrequencies ($\pi/2$ and $3\pi/2$ respectively) and the 1st vertical eigenfrequency of the soil layer for the translational stiffness component.
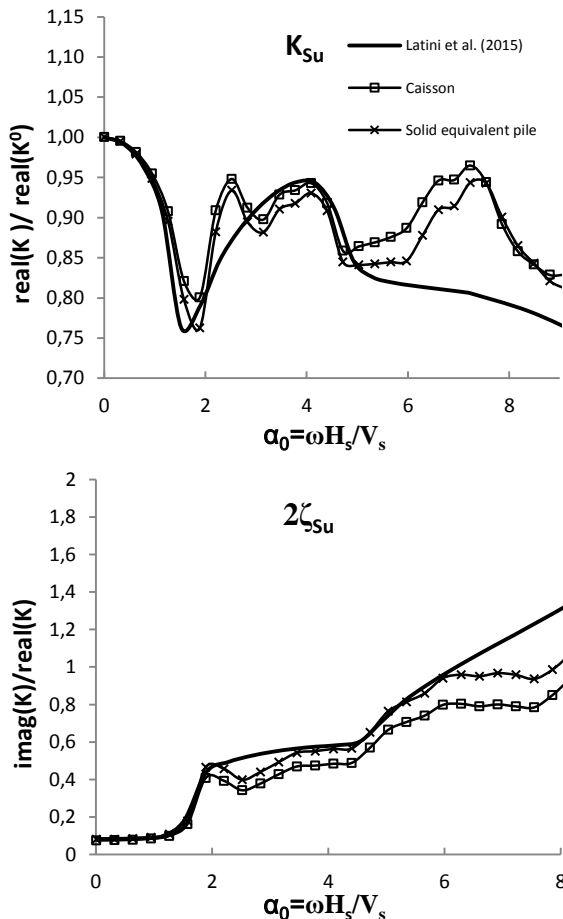

Figure 7 Variation of the translational stiffness and damping coefficients with respect to the dimensionless frequency for profile 2.

While, it seems that the coupling and the rocking stiffness terms are less sensitive to the 1st vertical resonance.
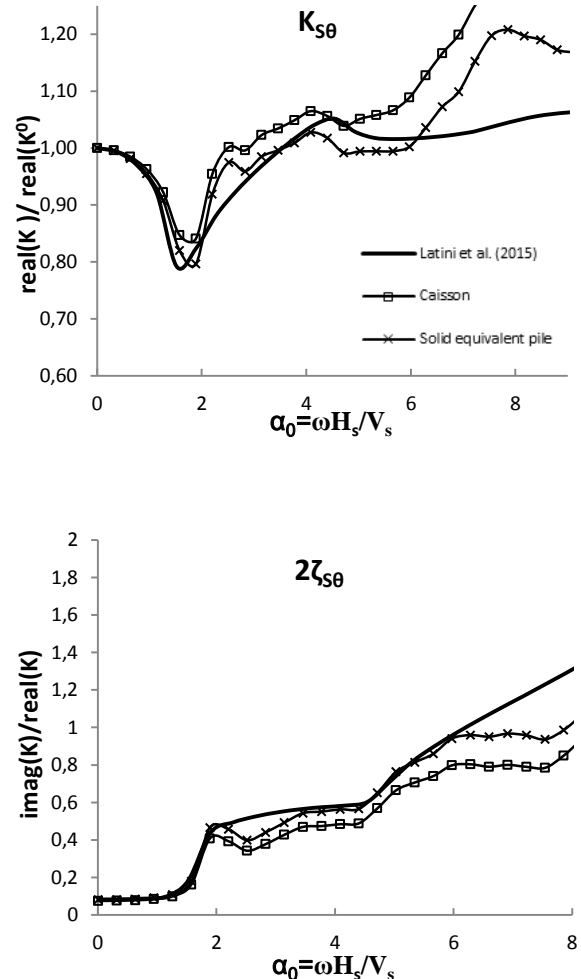

Figure 8 Variation of the coupling stiffness and damping coefficients with respect to the dimensionless frequency for profile 2.

In addition, they are characterized of an increase of stiffness approaching the 3rd eigenfrequency of the soil layer ($\alpha_0 = 5/2\pi$).

It is evident from the graphs that the dynamic response of the caisson is similar to the one of the solid equivalent pile, clearly for the translational and the rocking stiffness components. Furthermore, the analytical solution shows good agreement with the numerical results up to $\alpha_0 = 5$.

The imaginary part of the dynamic component is also shown in Figures 7, 8 and 9. The radiation damping exhibits a step variation in the frequency range, where the slope changes after each eigenfrequency of

the soil layer. This observation is consistent to previous studies on floating piles (Latini et al., 2015). Furthermore slightly higher damping is associated with the solid pile compared to the caisson.
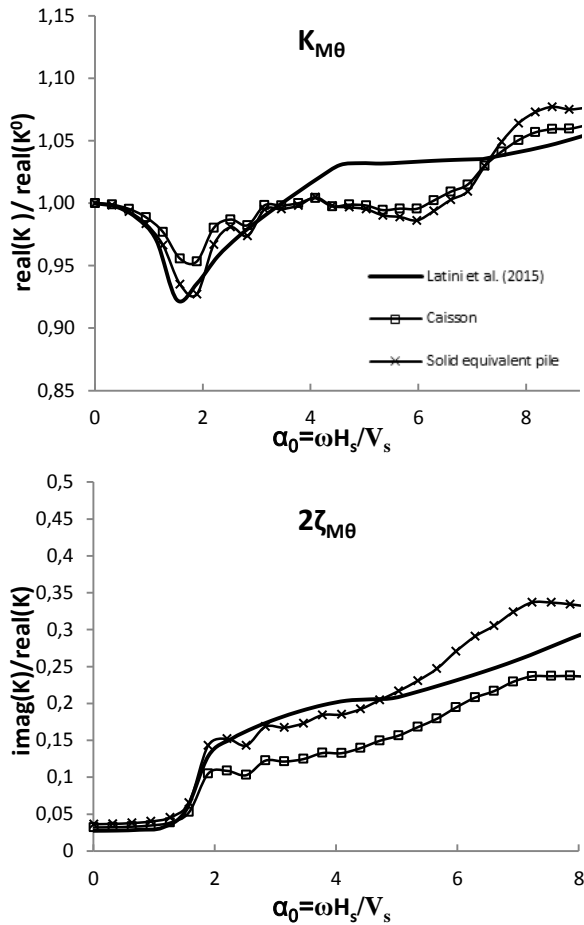
$K_{M\theta}$

$2\zeta_{M\theta}$

Figure 9 Variation of the rocking stiffness and damping coefficients with respect to the dimensionless frequency for profile 2.

In Figure 10, 11 and 12 the real (K_{su}, $K_{s\theta}$, and $K_{m\theta}$) and the imaginary ($2\zeta_{su}$, $2\zeta_{s\theta}$, and $2\zeta_{m\theta}$) parts of the dynamic impedances are presented for different values of the shear wave velocity of the soil layer (V_s=250-400m/s).
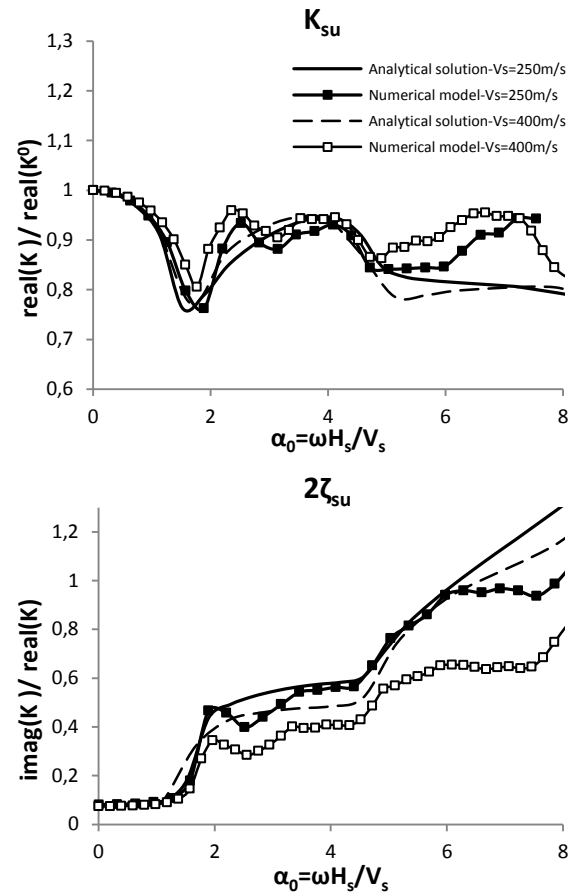
K_{su}

$2\zeta_{su}$

Figure 10 Variation of the translational stiffness and damping coefficients with respect to the dimensionless frequency. Effect of the soil stiffness on the real component and the imaginary component.

The same values as in the reference case are kept for the height of the foundation and the soil layer. Slightly scattered results are obtained by increasing the shear wave velocity of the soil layer. In addition, the drop of stiffness recorded at the first eigenfrequency of the soil layer is slightly more marked for medium soil profiles (V_s=250m/s). Moreover, it is noticed that the cross coupling and rocking stiffness coefficients exhibit higher values than the corresponding static component at higher frequencies.

Figure 12 Variation of the rocking stiffness and damping coefficients with respect to the dimensionless frequency. Effect of the soil stiffness on the real component and the imaginary component.
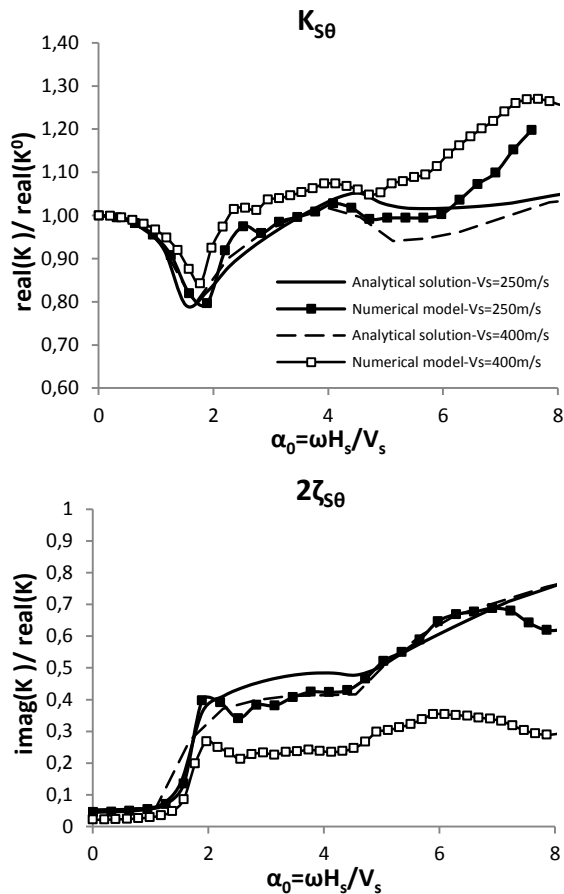

Figure 11 Variation of the coupling stiffness and damping coefficients with respect to the dimensionless frequency. Effect of the soil stiffness on the real component and the imaginary component.

In Figures 10, 11 and 12 the imaginary component is also illustrated for different values of the shear wave velocity of the soil layer. It is observed that increasing the stiffness of the soil or decreasing E_p/E_s the damping decreases. In addition, the radiation damping generated after the 1st eigenfrequency is almost zero for the rocking stiffness component. A significant offset is recorded comparing the numerical models with the analytical solution, when the stiffness of the soil layer is increased.
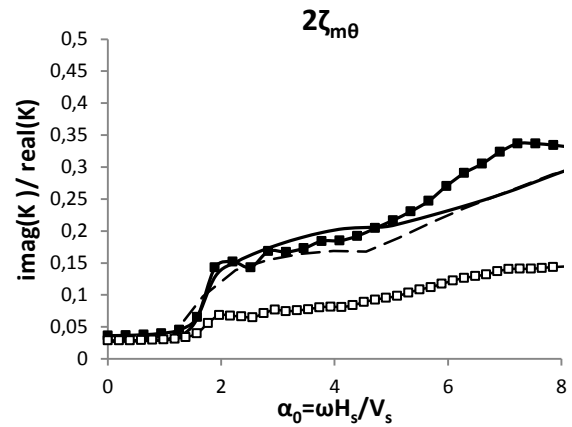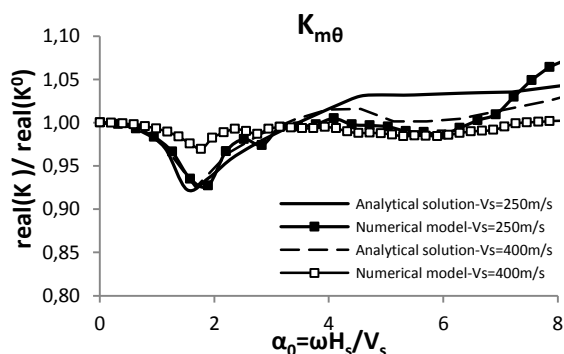

4 CONCLUSIONS

Numerical analysis is undertaken to investigate the dynamic response of suction caissons. The study also provides comprehensive comparison of the numerical models with existing analytical solutions formulated for piles. From the results of this study it seems that the general behavior of the suction caissons follows the trend of the analytical solution suggested by Novak and Nogami (1977) for piles. However for the caisson a Rayleigh wave is experienced in the inner soil with wave-length $\lambda = D$ in the high frequency range. In addition, the presence of the cap in the caisson design does not affect significantly the dynamic response of the soil-foundation system. The analytical formulation of Latini et al. (1977) provides good agreement with the numerical model of a caisson on a deep soil layer for frequencies up to $\alpha_0 = 5$. Concerning the effect of the soil stiffness on the dynamic impedances, it is noticed that decreasing V_s the damping increases, which it is in agreement with what observed in the analytical formulation. However at larger shear wave velocities a larger discrepancy between the numerical model and the analytical solution was observed. The effect of the inner soil in the dynamic response of the caisson appears more important for shallow soil formations than for deeper ones.

ACKNOWDLEGMENTS

5 REFERENCES

Adhikari, S., & Bhattacharya, S. (2012). Dynamic analysis of wind turbine towers on flexible foundations. Shock and vibration 19, 37-56.

Alexander, N.A. & Bhattacharya, S. (2011). The dynamics of monopole supported wind turbines in nonlinear soil. Proceedings of the 8th International Conference on Structural Dynamics (EURODYN 2011), Leuven, Belgium.

Bhattacharya, S. (2014). Challenges in design of foundations for offshore wind turbines. Institution of Engineering and Technology 10/2014.

Byrne, B.W.& Houlsby, G.T. (2006). Assessing novel foundation options for offshore wind turbines. World Maritime Technology Conference, London, UK.

DNV (2010). Offshore standard DNV-OS-J101: Design of offshore wind turbine structures. Technical report DNV-OS-J101, Det Norske Veritas.

Gazetas, G. (1984). Seismic response of end-bearing single piles. Soil Dynamics and Earthquake Engineering 3(2), 82–93.

Latini, C., Zania, V. & Johannesson, B. (2015) Dynamic stiffness and damping of foundation for jacket structures. Proceedings of 6th International Conference on Earthquake Geotechnical Engineering (6ICEGE 2015), Christchurch, New Zealand.

Liingard, M. (2006). Dynamic behavior of suction caissons. PhD Thesis. Aalborg University.

Mylonakis, G. (2001) Elastodynamic model for large diameter end-bearing shafts. Soils and foundations 41(3), 31-44.

Nogami, T. & Novak, M. (1977). Resistance of soil to a horizontally vibrating pile. Earthquake Engineering and Structural Dynamic 5(3), 249-261.

Novak, M. & Nogami, T. (1977) Soil-pile interaction in horizontal vibration. Earthquake engineering and structural dynamics 5, 263-281.

Nozoe H, Gyōten Y, & Fukusumi T. (1985) Dynamic analysis of a soil-pile system by the finite Fourier-Henkel transformation method – Case of a floating pile in horizontal vibration. Theoretical and applied mechanics 33, 377-392.

Simulia, D. S. (2013) Abaqus 6.13 User's Manual. Dassault Systems, Providence, RI.

Zania, V. (2014). Natural vibration frequency and damping of slender structures founded on monopiles. Soil dynamics and Earthquake engineering, 59, 8-20.